Unveiling Quasiperiodicity through Nonlinear Wave Mixing in Periodic Media

Alon Bahabad,[1] Noa Voloch,[2] and Ady Arie[1,*]

[1]School of Electrical Engineering, Wolfson Faculty of Engineering, Tel-Aviv University, Tel-Aviv 69978, Israel
[2]School of Physics and Astronomy, Raymond and Beverly Sackler Faculty of Exact Sciences, Tel-Aviv University, Tel-Aviv 69978, Israel

Ariel Bruner and David Eger

Electro-Optics Division, Soreq NRC, Yavne 81800, Israel
(Received 21 January 2007; published 14 May 2007)

Quasiperiodicity is the concept of order without translation symmetry. The discovery of quasiperiodic order in natural materials transformed the way scientists examine and define ordered structure. We show and verify experimentally that quasiperiodicity can be observed by scattering processes from a periodic structure, provided the interaction area is of finite width. This is made through a momentum conservation condition, physically realizing a geometrical method used to model quasiperiodic structures by projecting a periodic structure of a higher dimension.

DOI: 10.1103/PhysRevLett.98.205501 PACS numbers: 61.44.Br, 42.65.Ky, 42.70.Mp, 61.10.−i

The outcome of scattering processes by periodic media is diffraction—the generation of new waves at particular directions. There are numerous different kinds of such processes, e.g., electromagnetic optical waves diffracted from gratings, electrons diffracted from atomic crystals, etc. In all of these processes the condition for efficient generation of the scattered wave (diffraction condition) can be formulated in the form of momentum conservation: it needs to be satisfied only up to a reciprocal lattice vector (RLV) of the structure. Each such RLV can give rise to a different diffraction condition. We show that for a restricted-width interaction in which all beams propagate in the same direction within a periodic structure, momentum conservation can also be satisfied up to a projection of an RLV onto the direction of propagation. The real space description of this phenomenon entails projecting part of the structure defining lattice onto a line, but such a projection of a periodic lattice onto a subspace is a well-known scheme for the creation of quasicrystal models [1–3] (ordered but not periodic structures). As such, for certain propagation directions, the set of processes for which momentum conservation is satisfied exhibit quasiperiodic relations even though they take place within a periodic structure. We experimentally demonstrate this phenomenon using nonlinear wave mixing in a material with planar periodic modulation of $\chi^{(2)}$—its second-order nonlinear susceptibility, but it should be observable for any scattering process in which momentum conservation can be satisfied up to an RLV of some periodic lattice.

For second-order nonlinear optical interaction (nonlinear diffraction [4]), involving light beams with different frequencies, the condition of momentum conservation up to an RLV of the lattice is known as quasi-phase-matching (QPM) [5–8]: phase difference between interacting beams of different frequencies (due to dispersion) is compensated (phase-matched) using an appropriate nonlinear photonic crystal (NPC). Initially QPM was accomplished for a single process within a one-dimensional periodic NPC [7]. To phase match several processes there is a need for more complex structures such as periodic two-dimensional [8–11] or quasiperiodic [12–14]. However, in all of these structures, the given condition for phase matching is the existence of an RLV equal to the phase-mismatch vector $\mathbf{\Delta k}$. For a periodic two-dimensional NPC this condition [8,9,15] is written as $\mathbf{\Delta k} = m\mathbf{b_1} + n\mathbf{b_2}$, where $\mathbf{b_{1,2}}$ span the reciprocal lattice. The NPC itself is defined by some motif of positive or negative $\chi^{(2)}$ repeated at the vertices of some periodic lattice, over a $\chi^{(2)}$ reversed background. The lattice is spanned by the primitive vectors $\mathbf{a_{1,2}}$ which obey the orthogonality condition $\mathbf{a_i} \cdot \mathbf{b_j} = 2\pi\delta_{\mathbf{ij}}$. A second-order nonlinear interaction is actually a mutual interaction of three waves, i.e., a three-wave-mixing. When two such high amplitude waves (denoted as pump and idler) are directed into the NPC they give rise to a third wave, denoted as signal. Under plane-wave approximation this wave evolves according to [11]:

$$E_s(\Delta k_{x'}, \Delta k_{y'}) = \kappa \frac{1}{W} \iint_A d(x', y') \exp(ix'\Delta k_{x'} + iy'\Delta k_{y'}) dx' dy', \quad (1)$$

where κ is a constant depending on the pump and idler amplitudes and on the signal frequency and index of refraction. W is the width of a rectangular integration area A oriented along the signal propagation direction [as depicted in Fig. 1(a)]. $d(x', y') = \sum_{mn} \delta(\mathbf{r} - m\mathbf{a_1} - n\mathbf{a_2}) \otimes s_0(x', y')$ is the normalized spatial variation of the nonlinear coefficient $\chi^{(2)}$, where $s_0(x', y')$ is the motif geometrical representation (gets the value 1 inside the motif area and 0 otherwise), and $\otimes$ represents convolution. $\mathbf{\Delta k} = \Delta k_{x'}\hat{\mathbf{x}}' + \Delta k_{y'}\hat{\mathbf{y}}' = \mathbf{k_p} - \mathbf{k_s} - \mathbf{k_i}$ is the wave mismatch vector ($\mathbf{k_p}$, $\mathbf{k_s}$, and $\mathbf{k_i}$ are the wave vectors of the pump, signal, and idler,

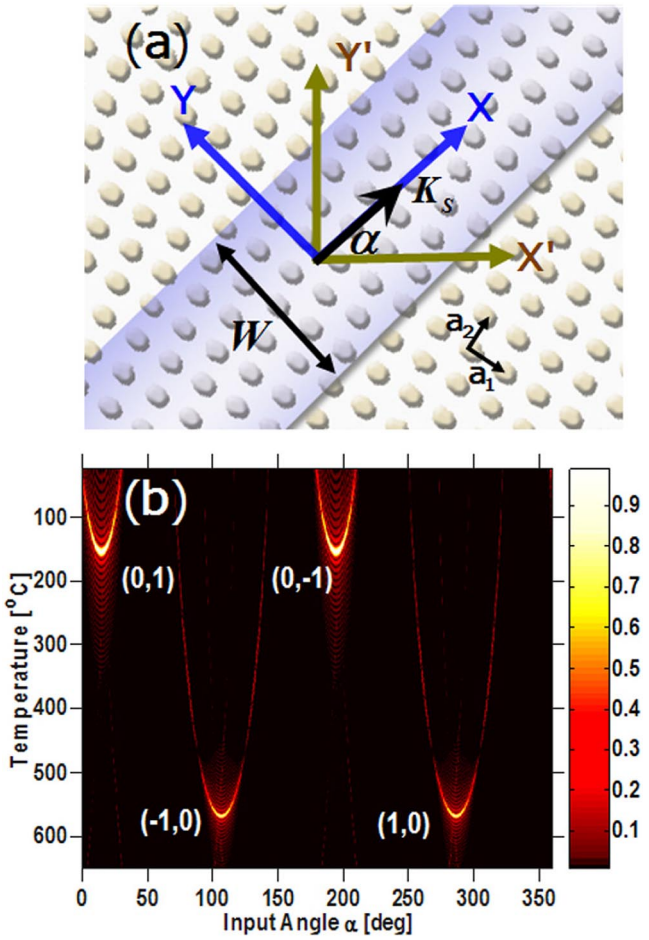

FIG. 1 (color online). Illustration of nonlinear optical lattice projection within an oblique NPC. (a) Restricted interaction area with respect to signal beam direction. (b) Calculation results of collinear projection-based SHG normalized intensity, as a function of input angle and material temperature.

respectively). Rotating to the (x, y) coordinate system we now consider only collinear radiation given by the condition $\Delta k_y = 0$. In addition, without any loss of generality, the integration limits in the x direction are extended to infinity. We also restrict the effective interaction width $W = y_1 - y_0$ which, up to diffraction limits, can be accomplished physically by either beam shaping or by a restricted area for $d(x', y')$. Equation (1) now reduces to

$$E_s(\Delta k_x) = \kappa \frac{1}{W} \int D(x) \exp(ix\Delta k_x) dx, \qquad (2)$$

where $D(x) = \int_{y_0}^{y_1} dy d(x, y) \equiv P_x d(x, y)$ is treated as a projection onto the x axis. We conclude that $E_s(\Delta k) = \kappa \frac{1}{W} \tilde{D}(\Delta k)$, where $\tilde{D}(\Delta k)$ is just the Fourier transform of $D(x)$ in the argument Δk (the x subscript was omitted as the problem reduces to one dimension).

Here we have an optical process which acts as a physical embodiment of lattice projection. This might be interesting as lattice projection is an important tool for the creation of quasicrystal models [1]. In fact, using generalizations of the arguments used previously by Zia and Dallas [16] for spectrum calculation of quasiperiodic structures, it can be shown that

$$\tilde{D}(\Delta k) = \frac{W}{A_{UC}} \times \sum_{mn} 2S_0\left(\frac{1}{2\pi}(mb_{1x'} + nb_{2x'}), \frac{1}{2\pi}(mb_{1y'} + nb_{2y'})\right) \times 2\pi \sum_{mn} \delta(\Delta k - M_{mn}) \mathrm{sinc}\left[\frac{WN_{mn}}{2}\right], \qquad (3)$$

where $\mathrm{sinc}(x) = \sin(x)/x$, $N_{mn} = (mb_{1y'} + nb_{2y'})\cos\alpha - (mb_{1x'} + nb_{2x'})\sin\alpha$, $M_{mn} = (mb_{1x'} + nb_{2x'})\cos\alpha + (mb_{1y'} + nb_{2y'})\sin\alpha$, and $A_{\mathrm{UC}} = |\mathbf{a_1} \cdot (\mathbf{a_2} \times \hat{\mathbf{z}})|$ is the lattice unit cell area. Equation (3) describes a distributed set of weighted Dirac delta functions (Bragg peaks) located at $\Delta k = M_{mn}$ with an associated Fourier coefficient $\rho_{mn} = \frac{W}{A_{\mathrm{UC}}} 2S_0 \mathrm{sinc}[\frac{W}{2} N_{mn}]$, where S_0 is the Fourier transform of $s_0(x', y')$ [17]. The above result gives the set of all collinear processes that can be phase matched in any periodic two-dimensional NPC, along with their anticipated efficiencies. This spectrum is not necessarily characteristic of a one-dimensional quasiperiodic structure, but it would be if we can draw a line parallel to $\mathbf{k}_s$ which passes through one and only one lattice point. As an example, if the NPC is built upon a cubic lattice with edges of unit length and the propagation direction is $\alpha = \mathrm{atan}(1/\tau)$, where $\tau = (1 + \sqrt{5})/2$ is the golden ratio, the processes that can be phase matched are those with $\Delta k_{mn} = 2\pi(m\tau + n)/(\sqrt{\tau + 2})$, which is the spectrum of the celebrated quasiperiodic Fibonacci tiling [18].

In general this spectrum contains more Bragg peaks than accounted for by the two-dimensional periodic lattice. This result is trivial when taking into account the sinc-type broadening of the Bragg peaks due to the finite interaction width, and the projection itself being reflected in k space by choosing $\Delta k_y = 0$. Each such "projected" peak can in principle be used to phase match a process with a phase-mismatch value equal to a projection of an RLV onto the direction of propagation. For the limiting case of $W \to \infty$ (plane-wave limit) we return to the Bragg peaks given along a line of the two-dimensional reciprocal lattice. To incorporate tolerances into the calculations, the interaction must be restricted to a finite crystal length L with the consequence of multiplying ρ_{mn} by $\mathrm{sinc}[\frac{L}{2}(\Delta k - M_{mn})]$ where Δk is the phase-mismatch value. But this additional factor accounts to any tolerance—for example, variation of wavelength or temperature would effect the phase-mismatch value, while angle tuning would change M_{mn} due to rotation of the propagation direction. In this regard, tolerance analysis for our purpose is no different than the known analysis carried for "standard" QPM [7].

To illustrate the analysis above, we calculate the behavior of a collinear second harmonic generation (SHG) process within an oblique lattice, with base vectors $\mathbf{a_1} = 6.2\ \mu\text{m} \angle -75°$, $\mathbf{a_2} = 7.4\ \mu\text{m} \angle 17°$ and with a hexagonal motif of 2.5 μm edges. This NPC was designed to phase match (through the coupling coefficient d_{33}) two collinear SHG processes of 1550 and 1047.5 nm at the same direction. For the 1047.5 nm SHG process, Fig. 1(b) shows the normalized amplitude of the second harmonic collinear radiation as a function of propagation direction and of temperature. The parameters taken were 10 μm interaction width and 0.2 cm interaction length [19]. Each parabola represents the contribution of a specific reciprocal lattice order, indicated near the parabola extremum point. Only the extremum points coincide with the regular plane-wave collinear phase-match condition—for $W \rightarrow \infty$ the parabolas diminish except for these points. On the other hand, letting (theoretically) $W \rightarrow 0$, the differences in efficiency between the standard and projection-based processes diminish.

To experimentally demonstrate the projection operation, we fabricated the above structure by using electric field poling [20] of a 1 cm long nonlinear crystal made of stoichiometric $LiTaO_3$ [21] [shown in Fig. 2(a)]. The phase-mismatch values for extraordinary polarized waves at room temperature are $\Delta k_1 = 2.97 \times 10^5\ \text{m}^{-1}$ and $\Delta k_2 = 8.20 \times 10^5\ \text{m}^{-1}$, respectively. The projection "arms" of the (0,1) and (1,0) QPM orders cross the pump propagation axis (the x axis) at the required phase-mismatch values for projection-based phase matching [see Fig. 2(b)]. For an ideal experiment we need to employ the unrealistic undiffracting top-hat beam profile; for adequate approximation low-diffraction beams must be used. When Gaussian beams are used, as in our experiment, better results can be achieved by restricting the significant contributing area of the nonlinear crystal to less than the beam waist (the nonlinear spatial modulation is restricted to a narrow strip) or, as was our choice, by aligning the setup so only part of the beam profile passes through a modulated area (while the whole beam is contained in the nonlinear media to exclude linear refraction). With a 1550 nm pump, we observed two SHG processes that are phase matched by the (1,0) QPM order, one directly by the RLV (when the pump enters at an angle of 3.4° with respect to the x direction), and the other is projection based (pump in the x direction). The two processes were captured by a CCD camera as shown in Fig. 3. The first process is the traditional phase matching process, where the generated second harmonic propagates in a −3.5° relative to the x axis. With pump waist radius of 20 μm (50 μm), the conversion efficiencies and spectral width are $3.5 \times 10^{-5}\ \text{W}^{-1}$ ($1.0 \times 10^{-5}\ \text{W}^{-1}$) and 20 nm (11 nm). The projection-based process is collinear, and exhibit different efficiencies and spectral widths: for waist radius of 20 μm (50 μm) we observed $2.6 \times 10^{-6}\ \text{W}^{-1}$ ($7.2 \times 10^{-7}\ \text{W}^{-1}$) and 3 nm (2.3 nm). The measurements were compared with a nu-

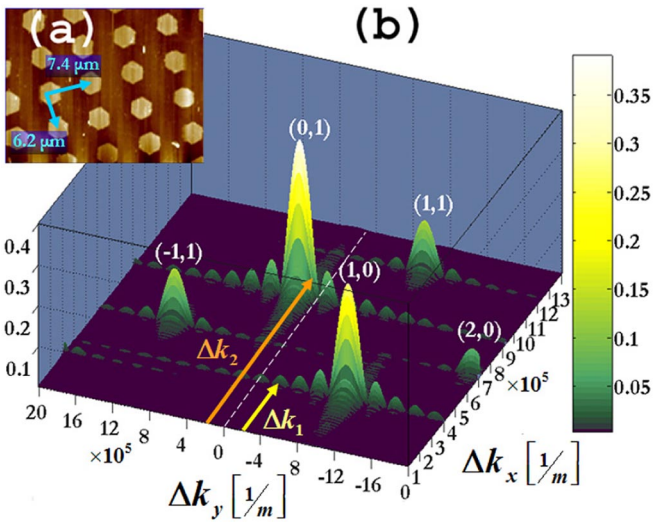

FIG. 2 (color online). NPC designed for dual phase matching of two SHG processes in the same direction. (a) AFM scan of the NPC. (b) Projection scheme upon the reciprocal lattice using plane-wave analysis: Fourier coefficients as a function of phase mismatch. The dashed white line indicates collinear QPM condition for beams propagating along the x axis. The short arrow indicates the projection of the (1,0) RLV, compensating Δk_1. The long arrow indicates the projection of the (0,1) RLV, compensating Δk_2.

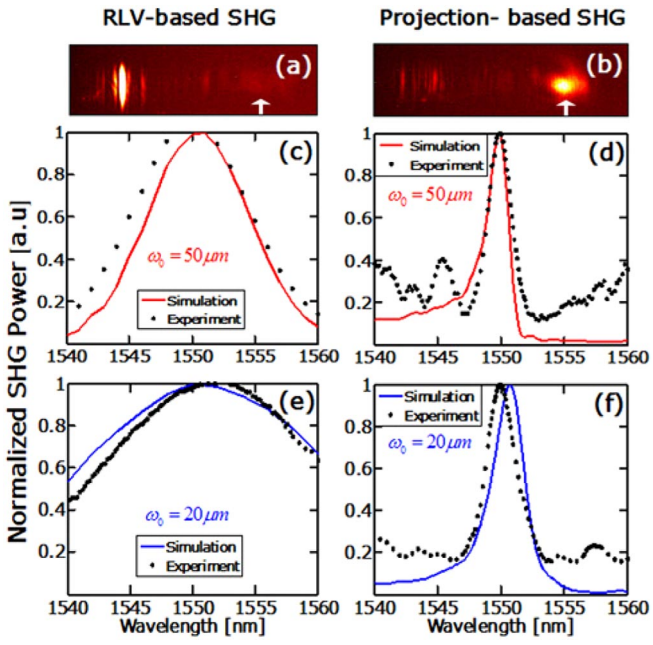

FIG. 3 (color online). Standard RLV-based noncollinear and collinear projection-based SHGs evolved from the same (1,0) QPM order. Panels (a)–(b): CCD caption of the standard RLV-based second harmonic (pump position is indicated by the white arrow) and of the projection-based second harmonic, respectively. Panels (c)–(e): Normalized experiment and simulation data for second harmonic power as function of wavelength.

merical simulation (employing split step Fourier method [22]) in which the nonlinear polarization induced by an undepleted Gaussian pump wave was used as a source for generating the second harmonic wave, while half of the beam profile passes through a modulated area. The simulated spectral widths are similar to those measured, as shown in Fig. 3. The effective interaction length for the noncollinear processes is smaller than for the collinear process as the interaction cross section between the pump and the inclined second harmonic is reduced. In view of the tolerance factor mentioned above, this results in a larger spectral aperture than for the collinear process. The calculated efficiencies are 3.6×10^{-6} W^{-1} (7.0×10^{-7} W^{-1}) for waist of 20 μm (50 μm). Theoretical efficiency calculation for the collinear radiation was made by using the Boyd-Kleinman formalism for focused Gaussian beams propagating within a homogeneous nonlinear crystal [23] modified to include the relevant $|\rho_{mn}|^2$ [Eq. (3)] factor (calculated for a $W = 2\omega_0$ interaction width). The resulting efficiencies are 1.3×10^{-6} W^{-1} (3.0×10^{-7} W^{-1}) for waist radius of 20 μm (50 μm). We also observed SHG for 1047.5 nm pump. In this case, for the RLV-based phase matching, the process is noncollinear with a 1° walk-off angle. The difference between the nominal input (output) angles for the projection-based and RLV-based processes is only 0.35° (0.7°), which is below the diffraction angle of the pump (second harmonic) beam. Hence, the two different processes could not be separated (using wide enough beams for angular separation would render the projection-based process efficiency 4 orders of magnitude smaller and extremely hard to detect). It should be emphasized that both SHG of 1047.5 and 1550 nm were phase matched at the same propagation direction (x axis), thus exhibiting quasiperiodic behavior (the phase-mismatch values for the two processes are incommensurate for all practical purposes) within a periodic lattice.

This phenomenon in which radiation is built along a certain direction by conserving momentum using an RLV component along the propagation direction, which in turn can be used to reveal quasiperiodicity, should not be restricted to nonlinear three-wave-mixing as was observed in our experiment. The same reasoning should apply to any scattering processes in which momentum conservation is satisfied up to an RLV of some lattice. Considering, for example, x-ray diffraction or diffraction from a (linear) photonic crystal, the $\Delta k_y = 0$ condition required for the projection operation is interpreted as measuring the diffracted radiation along the incident beam direction [24]. In our experiment separating the input beam from the output signal relied on their frequency difference. For diffraction, a backward propagating diffracted wave can be separated from the incident wave using a beam splitter. Structure analysis applications can come to mind when considering that this type of collinear radiation carries with it structure information of the transverse as well of the longitudinal dimensions although the process itself is characterized one-dimensionally (along a line). In addition, the strong dependency on the interaction width can be used to detect longitudinal defects.

This work was partly supported by the Israeli Science Foundation, Grant No. 960/05.

*Electronic address: ady@eng.tau.ac.il

[1] M. Senechal, *Quasicrystals and Geometry* (Cambridge University Press, Cambridge, England, 1995).
[2] M. Duneau and A. Katz, Phys. Rev. Lett. **54**, 2688 (1985).
[3] V. Elser, Phys. Rev. B **32**, 4892 (1985).
[4] I. Freund, Phys. Rev. Lett. **21**, 1404 (1968).
[5] J. A. Armstrong, N. Bloembergen, J. Ducuing, and P. S. Pershan, Phys. Rev. **127**, 1918 (1962).
[6] N. Bloembergen and A. J. Sievers, Appl. Phys. Lett. **17**, 483 (1970).
[7] M. M. Fejer, G. A. Magel, D. H. Jundt, and R. L. Byer, IEEE J. Quantum Electron. **28**, 2631 (1992).
[8] V. Berger, Phys. Rev. Lett. **81**, 4136 (1998).
[9] N. G. R. Broderick, G. W. Ross, H. L. Offerhaus, D. J. Richardson, and D. C. Hanna, Phys. Rev. Lett. **84**, 4345 (2000).
[10] S. Saltiel and Y. S. Kivshar, Opt. Lett. **25**, 1204 (2000).
[11] S. M. Russell, P. E. Powers, M. J. Missey, and K. L. Schepler, IEEE J. Quantum Electron. **37**, 877 (2001).
[12] S.-N. Zhu, Y.-Y. Zhu, and N.-B. Ming, Science **278**, 843 (1997).
[13] K. Fradkin-Kashi, A. Arie, P. Urenski, and G. Rosenman, Phys. Rev. Lett. **88**, 023903 (2001).
[14] R. Lifshitz, A. Arie, and A. Bahabad, Phys. Rev. Lett. **95**, 133901 (2005).
[15] Y. Glickman, E. Winebrand, A. Arie, and G. Rosenman, Appl. Phys. Lett. **88**, 011103 (2006).
[16] R. K. P. Zia and W. J. Dallas, J. Phys. A **18**, L341 (1985).
[17] Note that Eq. (3) can be written alternatively using the RLV $\mathbf{B}_{mn} = m\mathbf{b}_1 + n\mathbf{b}_2$, in which case M_{mn} and N_{mn} are simply the components of this vector after subjecting it to a rotation transformation of $(-\alpha)$ radians.
[18] R. Lifshitz, J. Alloys Compd. **342**, 186 (2002).
[19] For visualization purposes these parameters are different than the ones used in the experimental procedure.
[20] M. Yamada, N. Nada, M. Saitoh, and K. Watanabe, Appl. Phys. Lett. **62**, 435 (1993).
[21] A. Bruner, D. Eger, M. B. Oron, P. Blau, M. Katz, and S. Ruschin, Opt. Lett. **28**, 194 (2003).
[22] G. P. Agrawal, *Nonlinear Fiber Optics* (Academic, New York, 2001).
[23] G. D. Boyd and D. A. Kleinman, J. Appl. Phys. **39**, 3597 (1968).
[24] We consider such phenomena kinematically, assuming the diffraction pattern is proportional to the Fourier transform of the scattering media, while neglecting dynamical effects—see, for example,—F. Duan and J. Guojun, *Introduction to Condensed Matter Physics* (World Scientific, Singapore, 2005), Vol. 1.